Magnetic Resonance Imaging 62 (2019) 242–248

Contents lists available at ScienceDirect

Magnetic Resonance Imaging

journal homepage: www.elsevier.com/locate/mri

Original contribution

Accuracy of multi-parametric breast MR imaging for predicting pathological complete response of operable breast cancer prior to neoadjuvant systemic therapy

Hiroko Tsukada[a,b,*], Jitsuro Tsukada[c], Simone Schrading[a], Kevin Strobel[a], Takahiro Okamoto[b], Christiane K. Kuhl[a]

[a] Department of Diagnostic and Interventional Radiology, Hospital of the University of Aachen, RWTH, Pauwelsstrasse 30, 52074 Aachen, Germany
[b] Department of Surgery II, School of Medicine, Tokyo Women's Medical University, 8-1, Kawada-cho, Shinjuku-ku, 162-8666 Tokyo, Japan
[c] Department of Radiology, Nihon University School of Medicine, 30-1, Oyaguchi Kami-Cho, Itabashi-ku, 173-8610 Tokyo, Japan

A B S T R A C T

Objectives: To evaluate whether multiparametric breast-MRI, obtained before the initiation of neoadjuvant systemic therapy (NST) for operable breast cancer, predicts which cancer will achieve a pathological complete response (pCR) after the completion of NST.

Methods: This was an IRB-approved retrospective study on 31 consecutive patients (median age, 56 years) with operable invasive breast cancer (median size: 22 mm; triple-negative: 11/31 [35%], HER2-positive: 7/31 [23%], triple-positive: 13/31 [42%]) who underwent multiparametric DCE-MRI before the initiation of NST. The MRI protocol consisted of high-resolution dynamic contrast-enhanced MRI (DCE-MRI), T2-TSE, and DWI (b-values 0, 100, 800 s/mm^2). The results of surgical pathology after the completion of NST served as a standard of reference. Patient characteristics (age and menopausal status), pathological tumor characteristics (type, stage, nuclear grade, ER/PR and HER2 receptor status, and Ki-67 staining), and MRI characteristics (size, morphology, T2 signal intensity, enhancement kinetics, and ADC values) before NST were evaluated and compared between patients achieving pCR vs. non-pCR.

Results: Among 31 patients, 17 achieved pCR (55%) and 14 non-pCR (45%). No correlation was observed between patient- or tumor pathology-derived characteristics and pCR vs. non-pCR. Among MRI-derived tumor characteristics, tumor growth orientation parallel to Cooper's ligaments ($p = 0.002$) and wash-out rates ($p = 0.019$) correlated with pCR. Pre-NST ADC values were lower in patients achieving pCR ($P = 0.086$).

Conclusions: A tumor growth pattern parallel with Cooper's ligaments and a fast wash-out rate on pre-treatment multiparametric MRI are predictive of pCR and more closely associated with pCR than ADC values.

1. Introduction

Neoadjuvant systemic therapy (NST) is the standard treatment for local and advanced breast cancers. Indications for NST have recently been expanded to include small, operable breast cancers of specific molecular subtypes regardless of the tumor stage. Molecular subtypes are generally identified using immunohistochemical surrogate markers, specifically estrogen (ER), progesterone (PR), and human epidermal growth factor 2 (HER-2) receptors, and the proliferation marker Ki-67. In accordance with current clinical practice guidelines in Germany, all women with triple-negative breast cancers as well as all women with cancers exhibiting HER-2 receptors are offered NST [1,2] Accordingly, NST has two major purposes. The first purpose is to decrease tumor volume, which improves the operability of locally advanced breast cancer and increases the feasibility of breast-conserving surgery [3,4]. In operable breast cancer with triple-negative or HER2-enriched tumors, the purpose of NST is to assess sensitivity to systemic therapy. The usual metric to evaluate the chemosensitivity of breast cancer is the degree of regression after NST. Complete regression, or "a pathological complete response (pCR)", is associated with a good prognosis [5–8]. In spite of its advantages, NST for operable breast cancer is associated with a risk of "under-treatment" when cancer does not respond to systemic treatment. In that case, and because NST generally takes approximately two months to complete, a patient with biologically aggressive cancer may not receive an effective treatment over the course of several months, which increases the risk of tumor metastasis. Accordingly, there is a strong demand for methods beyond histological subtyping to improve the accuracy of predicted tumor responses to NST.

Dynamic contrast-enhanced magnetic resonance imaging (DCE-

* Corresponding author at: Department of Surgery II, School of Medicine, Tokyo Women's Medical University, 8-1, Kawada-cho, Shinjuku-ku, 162-8666 Tokyo, Japan.
E-mail address: tsukada.hiroko@twmu.ac.jp (H. Tsukada).

https://doi.org/10.1016/j.mri.2019.07.008
Received 30 April 2019; Received in revised form 12 July 2019; Accepted 13 July 2019

MRI) is widely used for breast cancer patients before surgery because of its high sensitivity for evaluating tumor extension, intraductal spread, and the presence of multicentric or multifocal disease [9,10]. Although previous studies reported that MRI findings after or during NST predict pCR [11–13], pCR predictions before the initiation of NST may be clinically advantageous for the planning of treatment strategies [14,15]. Although there have been some papers that reports correlation between baseline MRI and pCR by using advanced imaging protocols, such as a quantitative analysis or analysis with machine learning technique/computer-aided detection system [16–19], it is desirable that pCR can be predicted by a standard protocol generally obtained as preoperative clinical examination for breast cancer patients. However, to the best of our knowledge, only a few studies have evaluated whether MRI findings before NST predict pCR in breast cancer with a standard protocol [14,20–23].

The aim of the present study was to evaluate the predictive potential of pre-treatment MR imaging for operable breast cancer pCR to NST. We used baseline, pre-treatment MRI studies to investigate the relationships of tumor morphological features, signal intensities on T2-weighted images, and enhancement kinetics with post-treatment pCR, and compared these relationships with those of tumor-related as well as demographic features.

2. Materials and methods

2.1. Patients and data collection

Institutional Review Board approval was obtained for the present study and informed consent was obtained from all patients. Patients who had biopsy-proven primary invasive breast cancer scheduled for NST were included. All patients underwent DCE-MRI and received NST followed by surgery between October 2013 and July 2015. Patients were excluded if they did not undergo MRI prior to the initiation of NST or when the final results of surgical pathology were not available. We recorded the following tumor characteristics: histological type, nuclear grade, estrogen and progesterone receptor status, and HER-2/neu expression status, all of which were assessed by a qualified breast pathologist. In tumors with a questionable HER2 status, additional FISH tests were performed. T stages were identified prior to NST as the clinical stage (cT), which was based on all available clinical and imaging information obtained prior to beginning therapy. N stages were evaluated after sentinel node biopsy or axillary dissection prior to beginning NST.

To avoid repeated observations in the same patients confounding the results due to inter-lesion correlations, we only included the respective largest lesion in patients with multicentric cancer in the analysis.

2.2. MRI protocol

All patients underwent bilateral breast DCE-MRI on a clinical 1.5-T system (Intera; Philips Medical Systems) before beginning NST according to a standardized protocol. A double-breast, four-element surface coil (Invivo) equipped with a dedicated system to immobilize the breast in the cranio-caudal orientation (i.e. the slice-encoding direction for axial imaging) was used. The imaging protocol consisted of axial multislice 2-dimensional, gradient-echo, dynamic contrast-enhanced imaging (repetition time msec/echo time msec, 290/4.6 and the flip angle was 90°) performed prior to and four times after a bolus injection of gadobutrol (Gadovist, Bayer) at 0.1 mmol/kg body weight, followed by a saline flush, all injected at 3 mL/s. Images were acquired with a section thickness of 3 mm and a true (non-interpolated) acquisition matrix of 512 × 512. The field of view was adjusted to include both breasts, and ranged between 290 and 340 mm. T2-weighted TSE images were obtained without fat suppression and with exactly matching geometries. Diffusion-weighted images were obtained prior to the dynamic series as a single-shot spin-echo planar imaging sequence with diffusion-sensitizing gradients and b values of 0, 100, and 800 s/mm^2, an acquisition matrix of 260 × 258; a FOV and section thickness matching that of the dynamic series.

Image post-processing consisted of calculating apparent diffusion coefficient (ADC) maps, and the subtraction of all images of the post-contrast dynamic series.

2.3. MRI data analysis

All MR images were evaluated by experienced breast radiologists with 11 and 10 years of MRI experience who were blinded to the results of the treatment outcomes and used a dedicated workstation (IntelliSpace Portal, version 7.0; Philips Healthcare). Morphology, size, internal enhancement characteristics, internal architecture, tumor signal intensity (SI), time-SI curve patterns, and enhancement parameters were evaluated for all tumors according to the American College of Radiology BI-RADS 2013 5th edition. In addition to the BI-RADAS criteria, and in accordance with our institutional interpretation criteria for breast MRI, we evaluated a feature referred to as “tumor growth orientation” that denotes the main growth propagation of a breast tumor with respect to the direction of Cooper's ligaments. This feature is similar to that used in ultrasonography to describe growth orientation parallel or perpendicular to Cooper's ligaments [24,25].

Tumor shapes were classified as round/oval or irregular. Tumor margins were classified as circumscribed or non-circumscribed. The largest tumor diameter in two perpendicular directions was measured. Tumor internal enhancement characteristics were classified into four categories: homogeneous, heterogeneous, rim enhancement, or non-enhancing internal septations. The internal architecture was evaluated by assessing the tumor's SI on T2-weighted TSE images (T2WI). Tumor growth orientation was classified as being either parallel or perpendicular to local Cooper's ligaments. Since patients were in the prone position for axial imaging, Cooper's ligaments traveled from the back of the breast towards the nipple. Therefore, in most areas of the breast, growth orientation parallel to Cooper's ligaments indicated that the antero-posterior diameter of the tumor was longer than the medio-lateral diameter. In turn, growth orientation perpendicular to Cooper's ligaments suggested that the tumor medio-lateral diameter was broader than the antero-posterior diameter (Fig. 1).

All quantitative analyses were conducted on a dedicated workstation (IntelliSpace Portal, version 7.0, MR T1 Perfusion, Philips). ROIs were drawn manually on post-contrast images to locate the tumor, and subsequently copied to other pulse sequences. Care was taken to include only enhanced tumor tissue and account for possible phase shift effects on diffusion-weighted images. We assessed cancer SI on T2WI and mean, minimal, and maximal ADC.

In the analysis of enhancement kinetics, ROI-based time-SI curve patterns were plotted and categorized into three types (the persistent, plateau, or wash-out pattern) based on contrast-enhanced dynamic images. Moreover, maximum relative enhancement (MRE, as a percentage), the wash-in rate (per second), and wash-out rate (per second) were analyzed according to the following equation used by the IntelliSpace Portal, version 7.0, MR T1 Perfusion software:

$$MRE = (SIpeak - SIbaseline)/SIbaseline \times 100$$

where SIpeak represents the maximum SI after contrast medium administration, and SI baseline is the pre-contrast SI. The wash-in rate was automatically calculated as the maximum gradient of the SI change from the “time of arrival” to “time to peak”, with the time of arrival representing the arrival time of contrast medium into the ROI, and the time to peak as the time at which the maximum SI was reached. The

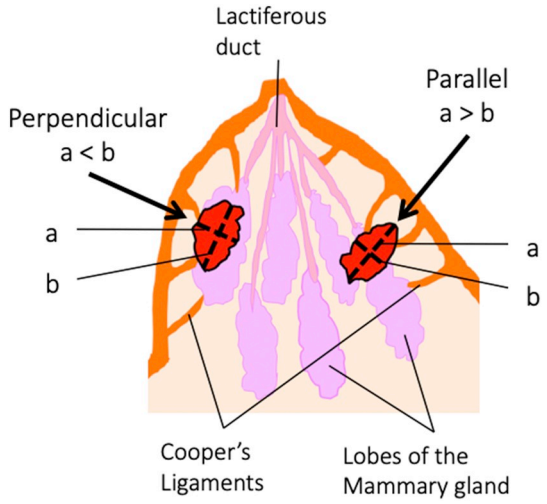

Fig. 1. Schematic drawing of tumor growth orientation.
Tumor growth orientation was classified as being either parallel or perpendicular to local Cooper's ligaments. The growth orientation parallel to Cooper's ligaments indicated that the antero-posterior diameter of the tumor (a) was longer than the medio-lateral diameter (b). In turn, the growth orientation perpendicular to Cooper's ligaments suggested that the tumor medio-lateral diameter (b) was broader than the antero-posterior diameter (a).

wash-out rate was automatically calculated as the maximum gradient of the SI change from "time to peak" until the end of dynamic imaging.

In data analyses, disagreements between the two readers were overcome by reviewing images together to reach a consensus.

2.4. Evaluation of pathological responses

Treatment responses were assessed by a histopathological examination of the final surgical specimen after the completion of NST. Regarding the definition of pCR, we used the definitions proposed by the Breast International Group and North American Breast Cancer Group; pCR is defined as the complete absence of invasive lesions and negative lymph node metastasis, regardless of the presence of ductal carcinoma in situ (DCIS) [26], [27].

2.5. Statistical analysis

Patient and tumor characteristics, such as age, menopausal status, clinical tumor stages, tumor grade, tumor subtypes, NST regimens, and morphological findings/enhancement parameters at DCE-MRI were compared between patients achieving pCR versus non-pCR. Medians and quartiles were used to describe continuous data. Fisher's exact test was used for all categorical data, and the Mann–Whitney *U* test was employed to compare MRI findings between pCR and non-pCR patients. In the analysis of tumor growth orientation as a predictor of pCR, sensitivity and specificity were calculated. Regarding continuous variables (ADC values and wash-out rates), a Receiver Operating Characteristics (ROC) analysis was performed to investigate their relationships with pCR, and the 95% confidence interval (CI) for the area under the curve (AUC) was calculated. All analyses were conducted using the SPSS 21.0 statistical software package (SPSS IBM). Interobserver agreement was evaluated by measuring the intraclass correlation coefficient. *P*-values of < 0.05 were considered to be significant.

Table 1
Patient and tumor characteristics ($N = 31$).

Parameters		Categories	pCR ($N = 17$)	Non-pCR ($N = 14$)	*P* value
			No. of patients (%)	No. of patients (%)	
Age		Range	30–69	30–75	0.204
		Median	50	59.5	
Menopausal		Pre	7 (41)	4 (28.6)	0.364
		Post	10 (59)	10 (71.4)	
Clinical tumor stage		cT1	9 (53)	6 (43)	0.422
		cT2	8 (47)	8 (57)	
		cN0	12 (70)	8 (57)	0.673
		cN1	4 (24)	5 (36)	
		cN2	1 (6)	0	
		cN3	0	1 (7)	
		M0	17 (100)	14 (100)	1.000
		M1	0	0	
Tumor grade		1	0	0	0.926
		2	7 (41)	6 (43)	
		3	10 (59)	8 (57)	
Subtype		Triple-positive	9 (53)	4 (29)	0.281
		Triple-negative	4 (23.5)	7 (50)	
		HER2-positive	4 (23.5)	3 (21)	
Ki67		Negative (< 20%)	3 (17.6)	4 (28.6)	0.671
		Positive (≥ 20%)	14 (82.4)	10 (71.4)	
NST	Triple-positive	TDM1 + TAM or AI	9 (52.8)	4 (28.6)	
	Triple-negative	NabPTX + GEM	2 (11.8)	4 (28.6)	1.000
		NabPTX + CBDCA	2 (11.8)	2 (14.3)	
		PTX + CBDCA	0	1 (7.1)	
	HER2-positive	PER + T + PTX	3 (17.7)	2 (14.3)	0.714
		PER + T	1 (5.9)	1 (7.1)	

Note. data are shown in numbers of patients with percentages in parentheses.
pCR = pathological complete response, c = clinical.
Triple-positive = ER positive and/or PR positive/HER2 positive.
Triple-negative = ER negative/PR negative/HER2 negative.
HER2 = human epidermal growth factor receptor 2.
HER2-positive = estrogen receptor (ER) negative/progesterone receptor (PR) negative/HER2 positive.
NST = neoadjuvand systemic therapy.
TDM1 = Trastuzumab emtansine, TAM = Tamoxifen, AI = Aromatase Inhibitors, NabPTX = Nab-Paclitaxel.
GEM = Gemcitabine, CBDCA = Carboplatin, PTX = Paclitaxel, PER = Pertuzumab, T = Trastuzumab.

3. Results

3.1. Patient cohort

Thirty-one cancers from 31 patients were included in the analysis. The demographic characteristics of patients and invasive breast cancers are shown in Table 1. In accordance with current clinical practice guidelines for NST for operable breast cancer, all patients had cancers corresponding to the following specific molecular subtypes: triple-negative cancer (ER/PR negative, HER2-negative) in 11/31 (35%), HER2-enriched in 7/31 (23%), and triple-positive cancers (ER and/or PR positive, and HER-2 enriched) in 13/31 (42%). NST regimes for individual patients were selected based on molecular subtypes and are listed in Table 1.

After the completion of NST, 17/31 (55%) patients achieved pCR at surgical resection, and the remaining 14 were classified as having non-pCR (45%). Stratified by tumor subtypes, pCR was observed in 69% (9/13) of triple-positive, 36% (4/11) of triple-negative, and 57.4% (4/7) of HER2-positive breast cancers.

3.2. Relationships between clinicopathological features and pCR

No relationships were observed between median age, menopausal status, clinical stage, or histological grades and pCR rates. Furthermore, no relationship was noted between the tumor subtype and pCR rate (Table 1).

3.3. Relationship between breast MRI findings and pCR

Interobserver correlation coefficients ranged between 0.698 and 1.000, indicating strong agreement between the 2 reviewers ($P < 0.01$).

All cancers exhibited mass enhancement on MRI; none of the cancers exhibited non-mass enhancement. The relationship between the MRI findings of cancers and pCR is summarized in Table 2.

Two MRI-derivable features correlated with pCR: tumor growth orientation and the wash-out rate. Patients with cancers exhibiting a growth pattern in parallel to Cooper's ligaments were significantly more likely to achieve pCR ($P = 0.002$, Table 2) (Figs. 2 and 3). The sensitivity with which tumor growth orientation predicted pCR was 70.6% (12/17), while specificity was 85.7% (12/14). Wash-out rates were significantly higher in pCR than in non-pCR (1.09 vs. 0.5, $P = 0.019$). The ROC analysis was used to analyze wash-out rates as a predictor of pCR. The best wash-out rate cut-off value was 1.09, and the area under the ROC curve was 0.75 (95% CI, 0.533–0.885).

None of the remaining features assessed, including baseline tumor sizes, shapes, margins, internal architectures, SI on T2-weighted TSE, other features of enhancement kinetics, and mean ADC, were associated with pCR, namely, they did not significantly differ between patients achieving pCR vs. non-pCR. Mean ADC values were lower in patients achieving pCR (median $0.52 \times 10^{-3}\,mm^2/s$; range, $0.28–0.86 \times 10^{-3}\,mm^2/s$) than in those with non-pCR (median $0.62 \times 10^{-3}\,mm^2/s$; range, $0.39–1.76 \times 10^{-3}\,mm^2/s$), but were not significantly different ($P = 0.086$).

Based on the ROC curve analysis, the best ADC cut-off value was

Table 2
Comparison of MR findings between pCR and non-pCR (N = 31).

Parameters	Categories		pCR (N = 17)	Non-pCR (N = 14)	*P* value
			No. of Patients	No. of Patients	
Size (mm)	Maximum	Range	8.5–48	14–46	0.350
		Median	18	22.5	
	Perpendicular	Range	8–30	10–42	0.125
		Median	13	18.5	
SI	T1WI	Range	5400–14,810	6400–16,700	0.648
		Median	10,000	8955	
	T2WI	Range	5800–23,000	3900–22,000	0.843
		Median	9500	9850	
	DWI	Range	508–7930	1725–12,490	0.577
		Median	3770	4440	
	ADC-value ($10^{-3}\,mm^2/s$)	Range	0.28–0.86	0.39–1.76	0.086
		Median	0.52	0.62	
Shape	Round/Oval		10 (58.8)	11 (78.6)	0.106
	Irregular		7 (41.2)	3 (21.4)	
Margin	Circumscribed		4 (23.5)	2 (14.3)	0.429
	Not circumscribed		13 (76.5)	12 (85.7)	
Internal architecture	T2WI	Homogeneous	4 (23.5)	4 (28.6)	0.534
		Heterogeneous	13 (76.5)	10 (71.4)	
	Post contrast	Homogeneous	1 (5.9)	2 (14.3)	0.929
		Heterogeneous	10 (58.8)	6 (42.9)	
		Rim enhancement	6 (35.3)	6 (42.9)	
		Dark internal septations	0 (0)	0 (0)	
Growth direction	Parallel		12 (70.6)	2 (14.3)	0.002
	Perpendicular		5 (29.4)	12 (85.7)	
Curve type	Persistent		1 (5.9)	0 (0)	0.963
	Plateau		6 (35.3)	6 (42.9)	
	Washout		10 (58.8)	8 (57.1)	
Enhancement parameters	MRE (%)	Range	99.98–190.57	73.49–199.75	0.284
		Median	121.44	130.82	
	Washin rate (1/s)	Range	4.28–13.93	4.68–14.49	0.634
		Median	9.48	9.58	
	Washout rate (1/s)	Range	0–1.86	0–1.01	0.019
		Median	1.09	0.5	

Note. data are shown in numbers of patients with percentages in parentheses.
pCR = pathological complete response, SI = signal intensity, T1WI = T1-weighted images, T2 = T2-weighted images.
DWI = diffusion-weighted images, ADC = apparent diffusion coefficient, MRE = maximum relative enhancement.

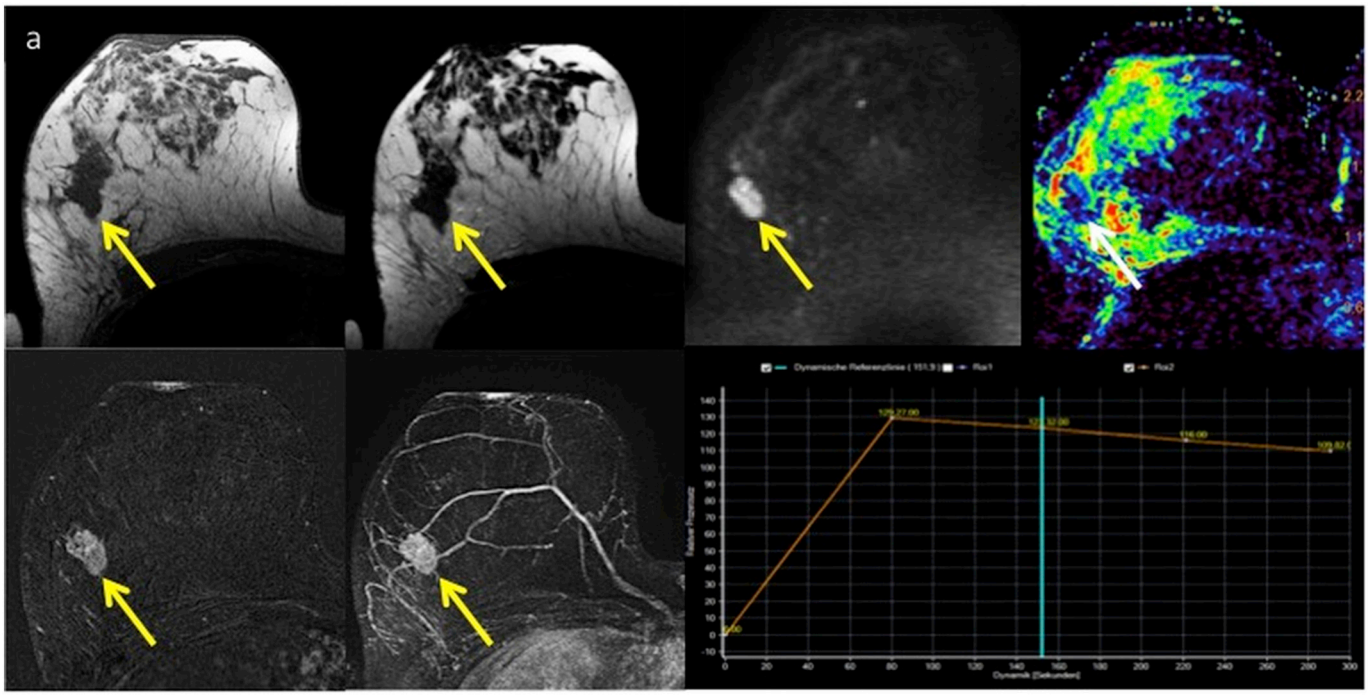

Fig. 2. MR images obtained from a 42-year-old woman with invasive carcinoma NST (no special type), clinical stage IIA, grade 2, who had pCR to NST. (a) Pre-contrast T1-weighted imaging (T1WI), (b) T2-weighted imaging (T2WI), and (c) diffusion-weighted imaging (b = 800 s/mm^2) revealed an oval-shaped, circumscribed mass in the lower outer quadrant of the right breast. The tumor showed a hypo-signal intensity on T1WI (a) and T2WI (b). The mean ADC value (d) in the tumor was 1.18×10^{-3} mm^2/s. A transverse dynamic contrast-enhanced T1-weighted subtraction MR image (e) and maximum intensity projection image of the early phase (f) showed strong early enhancement. The mass had parallel growth along Cooper's ligament (a-f, arrow). The time-signal intensity curve in the dynamic contrast-enhanced study demonstrated early strong enhancement and wash-out in the late phase of the dynamic series (g).

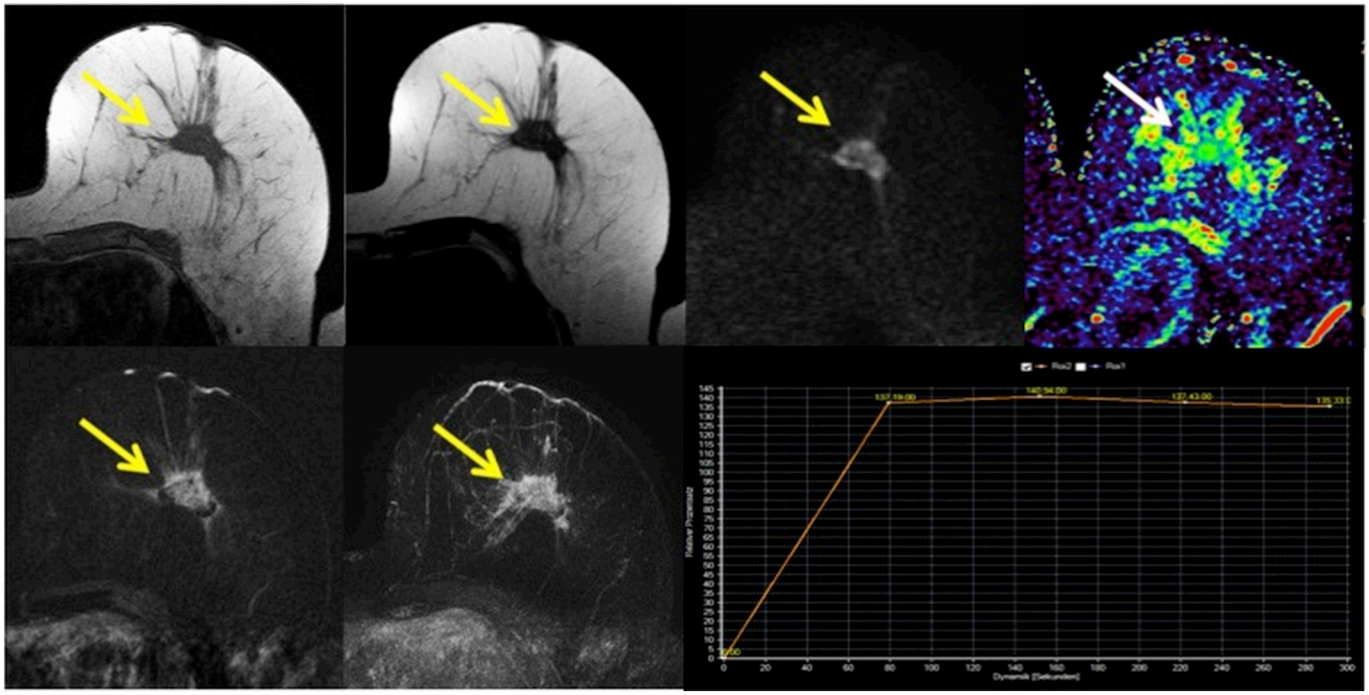

Fig. 3. MR images obtained from a 58-year-old woman with invasive NST cancer, clinical stage IIB, grade 3, who had non-pCR to NST. (a) Pre-contrast T1-weighted imaging (T1WI), (b) T2-weighted imaging (T2WI), and (c) diffusion-weighted imaging (b = 800 s/mm^2) revealed an oval-shaped, non-circumscribed mass lesion in the lower outer quadrant of the left breast. The tumor had a hypo-signal intensity on T2WI (b). The cancer showed a strong restriction in diffusion with a mean ADC value (d) of 0.6×10^{-3} mm^2/s. The cancer exhibited perpendicular growth against Cooper's ligament. A transverse dynamic contrast-enhanced T1-weighted subtraction MR image (e) and maximum intensity projection image (f) of the early phase showed strong early enhancement of the cancer. The time signal intensity curve revealed early enhancement in the early phase and a plateau-shaped curve (g).

0.55 mm^2/s, and the area under the ROC curve was 0.65 (95% CI, 0.415–0.831).

4. Discussion

Our results on multiparametric breast MRI in patients with operable breast cancer before the initiation of contemporary NST indicate that two distinct MRI-derivable features correlate with the prediction of pCR after treatment. A morphological tumor feature, i.e. tumor growth pattern parallel to Cooper's ligaments, and a tumor feature derived from enhancement kinetics, i.e. a high wash-out rate, were predictive of a patient's likelihood to achieve pCR. These findings are obtained with standard imaging protocols as breast MRI and do not require special hardware, software, or expertise to perform. Therefore, these MRI findings are thought to be clinically useful. Other MRI-derivable features assessed, such as tumor shapes, margins, internal enhancement architectures, T2 SI, and tumor ADC, did not differ significantly between patients achieving pCR vs. non-pCR. Moreover, neither demographic, histological or immunohistochemical features, nor baseline tumor size or stages correlated with pCR, indicating that pre-treatment MRI provides predictive information that is independent of and not obtainable by other information on individual patients, the cancer subtype, or stage.

An increasing number of operable breast cancers with specific receptor profiles undergo NST. The aim is to use local responses to treatment as a surrogate marker for the respective treatments' systemic efficacies. A complete pathological local response at the site of a tumor is a powerful surrogate for long-term systemic control, and, thus, a powerful prognostic and predictive endpoint. To improve patient stratification and avoid ineffective treatment decisions, it is highly desirable to be able to predict, before the initiation of NST, whether a given cancer is likely to respond and achieve pCR.

The vast majority of studies investigating the utility of breast MRI for predicting pCR to NST used MRI to assess responses either at the completion of NST, prior to surgery, or early after its initiation [11–13,28,29]. Fewer studies have evaluated the predictive power of breast MRI prior to initiation of NST. Nagashima et al. reported that the SI ratio and early contrast uptake on contrast-enhanced MRI before NST were significantly higher in what were classified as “chemosensitive” vs. “chemoresistant” groups [30]. Moreover, mass lesions and time-SI curve patterns with the wash-out type correlated with chemosensitive breast cancer [15]. However, in these studies, clinical responses, not pCR, were evaluated as the endpoint. To the best of our knowledge, some studies have been published that investigated the relationships between pre-treatment MRI findings and pCR in breast cancer [14,20,21]. In these studies, a round or oval shape [14,21], the wash-out slope [20] and wash-out curve type [31,32] on DCE-MRI were identified as predictive factors for pCR. In the present study, shape and morphology were not associated with pCR, whereas the cancer growth pattern was.

On pathophysiological grounds, it seems plausible that cancer growth patterns are associated with systemic treatment responses. Growth orientation may be a powerful criterion to evaluate a tumor's microarchitecture and influence on its micro-environment. Cancers that cross Cooper's ligaments may exhibit slower growth to cause a sufficient desmoplastic reaction. Cancers with a growth pattern parallel to Cooper's ligaments may exhibit faster and more expansive than infiltrative local growth. Therefore, additional assessments of tumor orientations in evaluations of tumor morphology may be useful for improving the prediction of pCR.

The present results are consistent with previous findings reported by Tsunoda et al. showing that carcinomas with an expansive growth pattern and relatively well-defined margins correlated with pCR [21]. In that study, “a relatively well-defined expansively growing tumor” was evaluated with a tumor shape and margin using images from ultrasonography and CT or MRI.

The present results also confirmed previous findings because wash-out rates were higher in patients achieving pCR vs. non-pCR [15,20]. Dongfeng et al. reported that the signal enhancement ratio (SER), which measures the wash-out slope based on SIs at three time points, correlated with pCR [20]. A possible explanation for the relationship between wash-out and responsiveness to treatment may be effective local drug delivery [32,33]. Previously, two studies reported that wash-out curve type on baseline DCE-MRI was significantly associated with pCR [31,32]. In the present study, a qualitative assessment of the shape of time/SI curve, i.e., the presence or absence of a wash-out curve type, did not correlate with pCR, whereas the quantitative feature “wash-out rate” did. The wash-out rate reflects the maximum gradient of the SI change regardless of the duration of the delayed phase. Accordingly, the wash-out rate is independent of the actual timing of the dynamic series, which may differ between institutions and patients; published values vary between 4 and 10 min [15,20,32]. The use of a quantitative parameter, i.e., the wash-out rate, instead of a qualitative description of the wash-out time course, may contribute to avoiding discrepancies in the evaluation of tumor wash-out characteristics.

ADC values were slightly lower in cancers achieving pCR vs. non-pCR. Previous findings on the utility of diffusion-weighted images for predicting responses prior to NST are conflicting. Park et al. reported that ADC values before NST were significantly lower in responders than in non-responders [34]. High ADC values indicate low cellularity tissue [35,36], which develops due to local necrosis secondary to hypoxia or because of local fibrosis/the desmoplastic components of cancer. Cancers with necrosis, fibrosis, or strong desmoplastic activity may be less chemosensitive, potentially due to impaired drug delivery because of the lack of perfusion and/or slow tumor growth in desmoplastic tumors. However, other studies did not confirm this relationship [37,38]. Thus, it remains controversial whether MRI ADC values before the initiation of treatment predicts NST chemosensitivity in breast cancer. The relatively small size of our study cohort may be the reason for lack of statistical power; however, since significant differences were noted in other features in our cohort, ADC values may be less powerful for predicting pCR than the growth pattern of tumors and wash-out rate.

The selection of the NST regimen has been suggested to influence the pCR rate. In the present study, no significant differences were observed in tumor subtypes or NST regimens between pCR and non-pCR (Table 1). Our pCR rates are consistent with previously reported response rates in patients with triple-positive, triple-negative, and HER2-positive breast cancers [39,40]. The most important limitation of the present study is the small size of the patient cohort. Furthermore, our cohort comprised patients with both the HER2-enriched and triple-negative subtypes of cancer undergoing targeted (HER2-blockade) and/or untargeted (chemotherapy alone) treatment. Previous studies on the utility of MRI for assessing responses to ongoing or completed neoadjuvant chemotherapy have shown that the prediction of pCR may vary with tumor subtypes. Moreover, our imaging protocol included non-fat-suppressed pulse sequences. A cancer's growth with respect to Cooper's ligaments may not be as readily assessed if protocols include fat-suppressed pulse sequences only. Another limitation is that all patients included in this study exhibited mass enhancement. Additional studies that include patients with non-mass lesions are needed to investigate the utility of pre-treatment MRI in these patients.

5. Conclusion

A growth pattern parallel to Cooper's ligaments and high wash-out rates on baseline, pre-treatment multiparametric DCE-MRI before NST

correlated with pCR in patients with HER2-enriched or triple-negative breast cancer. These results suggest that MRI prior to the initiation of NST may be clinically useful for predicting responses to NST.

References

[1] Kaufmann M, Hortobagyi GN, Goldhirsch A, Scholl S, Makris A, Valagussa P, et al. Recommendations from an international expert panel on the use of neoadjuvant (primary) systemic treatment of operable breast cancer: an update. J Clin Oncol 2006;24:1940–9.

[2] Buzdar AU. Preoperative chemotherapy treatment of breast cancer–a review. Cancer 2007;110:2394–407.

[3] Fisher B, Brown A, Mamounas E, Wieand S, Robidoux A, Margolese RG, et al. Effect of preoperative chemotherapy on local-regional disease in women with operable breast cancer: findings from national surgical adjuvant breast and bowel project b-18. J Clin Oncol 1997;15:2483–93.

[4] Makris A, Powles TJ, Ashley SE, Chang J, Hickish T, Tidy VA, et al. A reduction in the requirements for mastectomy in a randomized trial of neoadjuvant chemoendocrine therapy in primary breast cancer. Ann Oncol 1998;9:1179–84.

[5] Ferriere JP, Assier I, Cure H, Charrier S, Kwiatkowski F, Achard JL, et al. Primary chemotherapy in breast cancer: correlation between tumor response and patient outcome. Am J Clin Oncol 1998;21:117–20.

[6] Bear HD, Anderson S, Brown A, Smith R, Mamounas EP, Fisher B, et al. The effect on tumor response of adding sequential preoperative docetaxel to preoperative doxorubicin and cyclophosphamide: preliminary results from national surgical adjuvant breast and bowel project protocol b-27. J Clin Oncol 2003;21:4165–74.

[7] Rastogi P, Anderson SJ, Bear HD, Geyer CE, Kahlenberg MS, Robidoux A, et al. Preoperative chemotherapy: updates of national surgical adjuvant breast and bowel project protocols b-18 and b-27. J Clin Oncol 2008;26:778–85.

[8] von Minckwitz G, Untch M, Blohmer JU, Costa SD, Eidtmann H, Fasching PA, et al. Definition and impact of pathologic complete response on prognosis after neoadjuvant chemotherapy in various intrinsic breast cancer subtypes. J Clin Oncol 2012;30:1796–804.

[9] Rosen EL, Blackwell KL, Baker JA, Soo MS, Bentley RC, Yu D, et al. Accuracy of MRI in the detection of residual breast cancer after neoadjuvant chemotherapy. AJR Am J Roentgenol 2003;181:1275–82.

[10] Londero V, Bazzocchi M, Del Frate C, Puglisi F, Di Loreto C, Francescutti G, et al. Locally advanced breast cancer: comparison of mammography, sonography and Mr imaging in evaluation of residual disease in women receiving neoadjuvant chemotherapy. Eur Radiol 2004;14:1371–9.

[11] Minarikova L, Bogner W, Pinker K, Valkovic L, Zaric O, Bago-Horvath Z, et al. Investigating the prediction value of multiparametric magnetic resonance imaging at 3 t in response to neoadjuvant chemotherapy in breast cancer. Eur Radiol 2017;5:1901–11.

[12] Hylton NM, Blume JD, Bernreuter WK, Pisano ED, Rosen MA, Morris EA, et al. Locally advanced breast cancer: Mr imaging for prediction of response to neoadjuvant chemotherapy–results from Acrin 6657/i-spy trial. Radiology 2012;263:663–72.

[13] Xu HD, Zhang YQ. Evaluation of the efficacy of neoadjuvant chemotherapy for breast cancer using diffusion-weighted imaging and dynamic contrast-enhanced magnetic resonance imaging. Neoplasma 2017;64:430–6.

[14] Michishita S, Kim SJ, Shimazu K, Sota Y, Naoi Y, Maruyama N, et al. Prediction of pathological complete response to neoadjuvant chemotherapy by magnetic resonance imaging in breast cancer patients. Breast 2015;24:159–65.

[15] Uematsu T, Kasami M, Yuen S. Neoadjuvant chemotherapy for breast cancer: correlation between the baseline MR imaging findings and responses to therapy. Eur Radiol 2010;20:2315–22.

[16] Drisis S, Metens T, Ignatiadis M, Stathopoulos K, Chao SL, Lemort M. Quantitative DCE-MRI for prediction of pathological complete response following neoadjuvant treatment for locally advanced breast cancer: the impact of breast cancer subtypes on the diagnostic accuracy. Eur Radiol 2016;26:1474–84.

[17] Braman NM, Etesami M, Prasanna P, Dubchuk C, Gilmore H, Tiwari P, et al. Intratumoral and peritumoral radiomics for the pretreatment prediction of pathological complete response to neoadjuvant chemotherapy based on breast DCE-MRI. Breast Cancer Res. 2017;19:57.

[18] Ha R, Chin C, Karcich J, Liu MZ, Chang P, Mutasa S, et al. Prior to initiation of chemotherapy, can we predict breast tumor response? Deep learning convolutional neural networks approach using a breast MRI tumor dataset. J Digit Imaging 2018;25. https://doi.org/10.1007/s10278-018-0144-1. [Epub ahead of print].

[19] Cain EH, Saha A, Harowicz MR, Marks JR, Marcom PK, Mazurowski MA. Multivariate machine learning models for prediction of pathologic response to neoadjuvant therapy in breast cancer using MRI features: a study using an independent validation set. Breast Cancer Res Treat 2019;173:455–63.

[20] Dongfeng H, Daqing M, Erhu J. Dynamic breast magnetic resonance imaging: pretreatment prediction of tumor response to neoadjuvant chemotherapy. Clin Breast Cancer 2012;12:94–101.

[21] Tsunoda-Shimizu H, Hayashi N, Hamaoka T, Kawasaki T, Tsugawa K, Yagata H, et al. Determining the morphological features of breast cancer and predicting the effects of neoadjuvant chemotherapy via diagnostic breast imaging. Breast Cancer 2008;15:133–40.

[22] Shin HJ, Baek HM, Ahn JH, Baek S, Kim H, Cha JH, et al. Prediction of pathologic response to neoadjuvant chemotherapy in patients with breast cancer using diffusion-weighted imaging and MRS. NMR Biomed 2012;25:1349–59.

[23] Richard R, Thomassin I, Chapellier M, Scemama A, de Cremoux P, Varna M, et al. Diffusion-weighted MRI in pretreatment prediction of response to neoadjuvant chemotherapy in patients with breast cancer. Eur Radiol 2013;23:2420–31.

[24] Ko ES, Lee BH, Kim HA, Noh WC, Kim MS, Lee SA. Triple-negative breast cancer: correlation between imaging and pathological findings. Eur Radiol 2010;20:1111–7.

[25] Wojcinski S, Soliman AA, Schmidt J, Makowski L, Degenhardt F, Hillemanns P. Sonographic features of triple-negative and non-triple-negative breast cancer. J Ultrasound Med 2012;31:1531–41.

[26] Fumagalli D, Bedard PL, Nahleh Z, Michiels S, Sotiriou C, Loi S, et al. A common language in neoadjuvant breast cancer clinical trials: proposals for standard definitions and endpoints. Lancet Oncol 2012;13:e240–8.

[27] Sinn HP, Schmid H, Junkermann H, Huober J, Leppien G, Kaufmann M, et al. Histologic regression of breast cancer after primary (neoadjuvant) chemotherapy. Geburtshilfe Frauenheilkd 1994;54:552–8.

[28] Fangberget A, Nilsen LB, Hole KH, Holmen MM, Engebraaten O, Naume B, et al. Neoadjuvant chemotherapy in breast cancer-response evaluation and prediction of response to treatment using dynamic contrast-enhanced and diffusion-weighted MR imaging. Eur Radiol 2011;21:1188–99.

[29] Jensen LR, Garzon B, Heldahl MG, Bathen TF, Lundgren S, Gribbestad IS. Diffusion-weighted and dynamic contrast-enhanced MRI in evaluation of early treatment effects during neoadjuvant chemotherapy in breast cancer patients. J Magn Reson Imaging 2011;34:1099–109.

[30] Nagashima T, Sakakibara M, Nakamura R, Arai M, Kadowaki M, Kazama T, et al. Dynamic enhanced MRI predicts chemosensitivity in breast cancer patients. Eur J Radiol 2006;60:270–4.

[31] Woolf DK, Padhani AR, Taylor NJ, Gogbashian A, Li SP, Beresford MJ, et al. Assessing response in breast cancer with dynamic contrast-enhanced magnetic resonance imaging: are signal intensity-time curves adequate? Breast Cancer Res Treat 2014;147:335–43.

[32] Craciunescu OI, Blackwell KL, Jones EL, Macfall JR, Yu D, Vujaskovic Z, et al. DCE-MRI parameters have potential to predict response of locally advanced breast cancer patients to neoadjuvant chemotherapy and hyperthermia: a pilot study. Int. J. Hyperthermia 2009;25:405–15.

[33] Semple SI, Staff RT, Heys SD, Redpath TW, Welch AE, Ahearn TS, et al. Baseline MRI delivery characteristics predict change in invasive ductal breast carcinoma pet metabolism as a result of primary chemotherapy administration. Ann Oncol 2006;17:1393–8.

[34] Park SH, Moon WK, Cho N, Song IC, Chang JM, Park IA, et al. Diffusion-weighted MR imaging: pretreatment prediction of response to neoadjuvant chemotherapy in patients with breast cancer. Radiology 2010;257:56–63.

[35] Sugahara T, Korogi Y, Kochi M, Ikushima I, Shigematu Y, Hirai T, et al. Usefulness of diffusion-weighted MRI with echo-planar technique in the evaluation of cellularity in gliomas. J Magn Reson Imaging 1999;9:53–60.

[36] Lyng H, Haraldseth O, Rofstad EK. Measurement of cell density and necrotic fraction in human melanoma xenografts by diffusion weighted magnetic resonance imaging. Magn Reson Med 2000;43:828–36.

[37] Nilsen L, Fangberget A, Geier O, Olsen DR, Seierstad T. Diffusion-weighted magnetic resonance imaging for pretreatment prediction and monitoring of treatment response of patients with locally advanced breast cancer undergoing neoadjuvant chemotherapy. Acta Oncol 2010;49:354–60.

[38] Manton DJ, Chaturvedi A, Hubbard A, Lind MJ, Lowry M, Maraveyas A, et al. Neoadjuvant chemotherapy in breast cancer: early response prediction with quantitative MR imaging and spectroscopy. Br J Cancer 2006;94:427–35.

[39] Harbeck N, Gluz O. Neoadjuvant therapy for triple negative and her2-positive early breast cancer. Breast 2017;34(Suppl 1):99–103. https://doi.org/10.1016/j.breast.2017.06.038.

[40] Nakatsukasa K, Koyama H, Oouchi Y, Imanishi S, Mizuta N, Sakaguchi K, et al. Docetaxel, cyclophosphamide, and trastuzumab as neoadjuvant chemotherapy for her2-positive primary breast cancer. Breast Cancer 2017;24:92–7.